# Epoxy Resin–Polyethersulphone Blends

M. AKAY[1,*] and J. G. CRACKNELL[2]

[1]Department of Mechanical and Industrial Engineering, University of Ulster at Jordanstown, Newtownabbey, BT37 0QB, Northern Ireland, and [2]MTD, Shorts Brothers plc, Airport Road, Belfast, BT3 9DZ, Northern Ireland

SYNOPSIS

A series of amine-cured epoxy resin systems and the blends of these containing up to 50% polyethersulphone (PES) were evaluated in terms of curing behavior, microstructure, and mechanical and dynamic mechanical thermal properties. The epoxy networks were based on a 2 : 1 mixture of triglycidyl-*p*-aminophenol and the polyglycidylether of a phenol-formaldehyde novolac, and a curing agent of 3,3′-diaminodiphenylsulphone (DDS). The curing mechanism and the rate of curing were affected by the DDS and PES contents. Reaction between the epoxy resin and hydroxyl groups attached to PES was indicated in epoxy-rich formulations. Phase separation, evident in all the blends, was affected by the curing rate. Various blend morphologies were observed depending on the epoxy network/thermoplastic composition. Blending improved ductility and toughness-related properties, particularly at 20–40% PES contents, which corresponded to spinodal/co-continuous morphologies. Changes in glass transition behavior were attributed to possible variations in intermolecular free volume. © 1994 John Wiley & Sons, Inc.

## INTRODUCTION

Epoxy resins possess various attractive thermo-mechanical properties, but they are inherently brittle. Substantial ongoing research is directed toward improving the toughness and damage tolerance of epoxy resins and epoxy-based fiber composites. Blending with a high-performance engineering thermoplastic is one way of improving toughness. A clear understanding of such material systems requires evaluation of the component polymers as well as the blends for curing behavior, material structure, and mechanical performance.

Curing of an epoxy resin with an amine may result in four possible reactions: primary amine–epoxy (PA–E), secondary amine–epoxy (SA–E), hydroxyl–epoxy (E–OH), and epoxy–epoxy (E–E) polymerizations. The relative extents of the different reactions are mainly determined by the ratio of amine to epoxy groups[1] and the curing conditions.[2,3] These reactions could take place intermolecularly to form crosslinks or intramolecularly to form noncrosslinked ring structures or chain extensions. The resultant network structure is inevitably heterogeneous consisting of regions of varying degrees of crosslink densities.

The mechanical properties of thermoplastic-modified epoxy resins have been shown to depend on the crosslink density[4] of the resin as well as the morphology[5] of the phase separation within the blend and the strength of the interface[6] between the phases. Therefore, the subject requires a comprehensive study in order to include as many of the relevant parameters as possible.

This work reports on the curing behavior, morphology, and mechanical properties of the blends of polyethersulphone, a tough thermoplastic of high thermal stability, with various epoxy–amine resin systems. The aim of the study was to identify the types of chemical and physical interactions between the component polymers, to investigate microstructural features of the blends and any improvements in the mechanical behavior, and, where possible, to show correlations between these parameters.

* To whom correspondence should be addressed.

Journal of Applied Polymer Science, Vol. 52, 663–688 (1994)
 CCC 0021-8995/94/050663-26

## EXPERIMENTAL

### Synthesis

The raw materials used were triglycidyl-*p*-aminophenol (MY0510), 2.2 functionality glycidylether of a phenol-formaldehyde novolac (DEN431), 3,3′-diaminodiphenylsulphone (DDS) curing agent, and ICI polyethersulphone (PES) "Victrex 5003P." This is a low-molecular-weight ($\overline{M_n} \approx 20{,}000$) grade PES and is end-capped so that it contains hydroxyl groups.

Various epoxy formulations based on a 2 : 1 mixture of MY0510/DEN431 epoxy resins were investigated as a function of amine curing agent in the range of 34–75 phr DDS. The quantity of DDS may be more conveniently expressed as a fraction of the exact stoichiometric amount required for curing, thus, the DDS range considered here corresponds to a stoichiometric fraction range of 0.6–1.3. Approximately 58 phr DDS is required for the stoichiometric (i.e., DDS/epoxy = 1) cure of the epoxy resin mixture. The relevant calculations and the details of the chemical preparations are presented elsewhere.[7,8] Briefly, the epoxy resins were mixed in a waterbath at 90°C to reduce viscosity; curing agent was then added and mixed in thoroughly. The mixture was poured into open molds, degassed at 120°C, and cured at 180°C for 3 h.

The epoxy resin formulations at three different curing agent levels, viz. 46, 61, and 75 phr DDS (or 0.8, 1.05, and 1.3 DDS/epoxy ratios) were blended with PES at 10, 20, 30, 40, and 50% w/w PES concentrations. Each blend was prepared by dissolving the appropriate amount of PES in a mixture containing approximately 10% methanol and 90% dichloromethane at 90°C. One third of the methanol/dichloromethane was allowed to boil off prior to adding the resins at the required ratios. The resins and PES were mixed using a constant-speed mechanical stirrer until a further third of the remaining solvent mixture was boiled off. DDS was then added and mixing continued until the viscosity of the mixture showed a marked increase, indicating that most of the solvent had evaporated. The reagents were cast into molds, degassed in a vacuum oven at 145°C for 30 min, cured at 180°C for approximately 3 h, then cooled down slowly to room temperature.

Cured plaques were clear, amber brown in color and appeared optically homogeneous. The plaques had a surface area of 84 × 124 mm$^2$ and thicknesses of 2.5–3.2 mm. The variations in plaque thicknesses resulted from the open-mold casting.

### Test Methods

Calorimetric measurements were obtained using a DuPont DSC10 differential scanning calorimeter (DSC), in conjunction with a DuPont 2000 thermal analyst. The heat of reaction for various formulations was determined using isothermal DSC, which produces a continuous curve of the rate of heat generation (i.e., heat flow) for a given sample as a function of time. The reaction was considered complete when the rate curve leveled off to the baseline. After the completion of isothermal cure, the samples were cooled rapidly in the DSC to 90°C and then reheated to 335°C at 10°C/min in order to determine the residual heat of reaction. The sum of the isothermal and the residual heats of reactions was taken to represent the ultimate heat of cure, $\Delta H_T$, which was used to calculate the degree of conversion, $c = \Delta H_p / \Delta H_T$, and the rate of conversion, $dc/dt = (dH/dt)/\Delta H_T$, at a given time during the curing reaction. $\Delta H_p$ represents the partial heat of cure of the sample and $dH/dt$ the heat flow at a time $t$.

Dynamic mechanical data were obtained using a DuPont 983 dynamic mechanical analyzer (DMA) in resonant frequency mode over a temperature range −90–265°C and at a heating rate of 4°C/min up to room temperature and 2°C/min above room temperature. Test pieces were ~ 10 mm wide and the clamp separations were adjusted (8–20 mm) according to the stiffness of the specimens. Wider clamp settings were required for the stiffer and/or thicker specimens. The amplitude (peak-to-peak) of sinusoidal oscillations, mostly 0.45–1.00 mm, were also chosen according to the stiffness and thickness of the specimens. Some of the DMA specimens were postcured by being heated to 235°C at 1°C/min.

Tensile testing was performed using an Instron machine (model no. 6025), in accordance with ASTM D638M (the type M-II specimens) at a crosshead speed of 50 mm/min. The distance between the clamps was 50 mm and an extensometer of 12.5 mm gauge length was employed for strain measurements.

Notched specimens (~ 2.5 × 12 × 70 mm) were edge-on impact tested in three-point bending mode on a support span of 40 mm at 0.7 m/s using an instrumented falling weight machine fitted with a 45° chisel-shaped striker of 3 mm tip radius. Notches of approximately 2 mm depth were milled with a 45° cutter of 0.25 mm radius.

The fractured surfaces of the impact test pieces were mounted on stubs and coated with platinum-gold using a Polaron sputter coater and examined

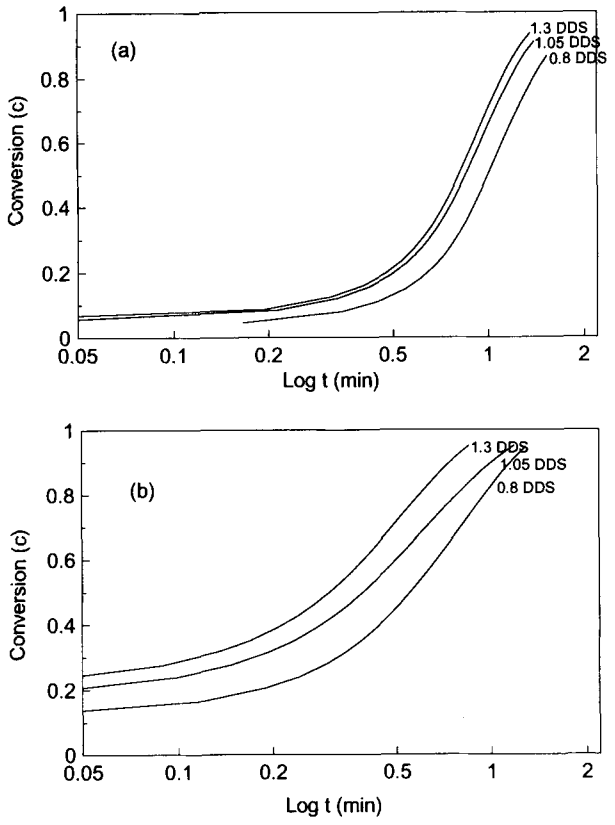


**Figure 1** Degree of conversion vs. log (time) for various DDS concentration at isothermal cure temperatures of (a) 170°C and (b) 200°C.

**Table I Ultimate Heat of Cure as a Function of Formulation and Cure Temperature**

| Cure Temperature (°C) | Heat of Cure (J/g) | | |
|---|---|---|---|
| | 0.8 DDS Epoxy | 1.05 DDS Epoxy | 1.3 DDS Epoxy |
| 145 | 616 | 601 | — |
| 150 | 621 | 613 | 652 |
| 155 | 617 | 592 | 574 |
| 160 | 657 | 596 | 608 |
| 165 | 670 | 577 | 598 |
| 170 | 610 | 626 | 645 |
| 180 | 672 | 607 | — |
| 190 | — | 663 | 592 |
| 200 | 685 | 637 | 555 |
| 210 | 663 | 599 | 575 |

by scanning electron microscopy (SEM) using a Jeol JSM6400. Some of the blend specimens were acid etched prior to sputter coating in order to remove the thermoplastic component.

The morphology of the blends was studied by transmission electron microscopy (TEM) using a Jeol JEM100S instrument at an accelerating voltage of 60 kV. Approximately 0.1-$\mu$m sections were microtomed from the moldings at room temperature using an LKB ultra-microtome fitted with a dia-

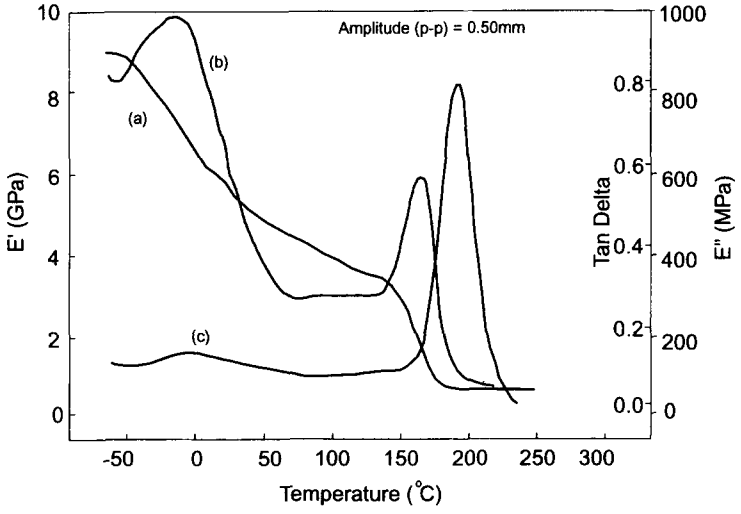


**Figure 2** Dynamic mechanical traces for 1.0 DDS epoxy resin: (a) real modulus ($E'$), (b) loss modulus ($E''$), and (c) tan $\delta$.

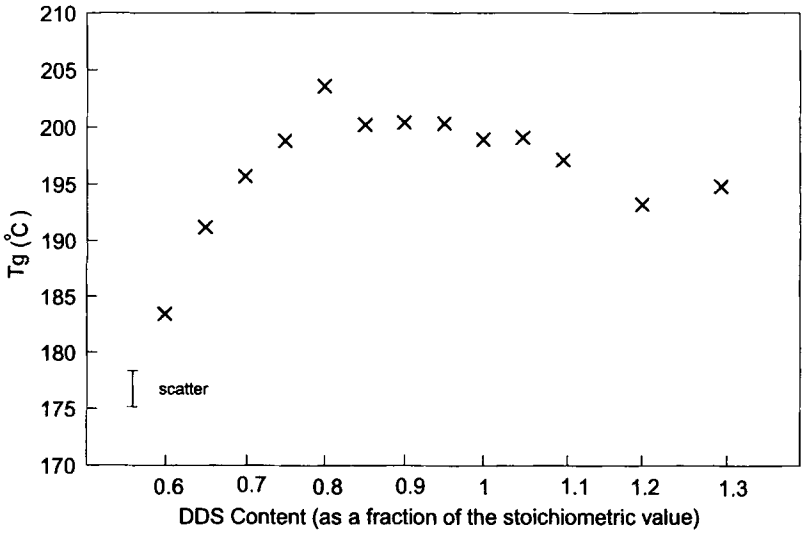


**Figure 3** Variation of the glass transition temperature of the epoxy network with the DDS concentration.

mond knife. The sections were mounted on copper grids for TEM.

Tensile and impact tests were conducted at ambient temperature and the results presented are an average of at least five measurements for these tests and three measurements for dynamic mechanical tests. A scatter band is indicated where the variation in data is appreciable.

## RESULTS AND DISCUSSION

### Epoxy–Amine Formulations

The curing behavior of various epoxy–amine systems was compared using isothermal DSC. The data are presented in Figure 1 and Table I and show that the degree of conversion, $c$, increases with increasing

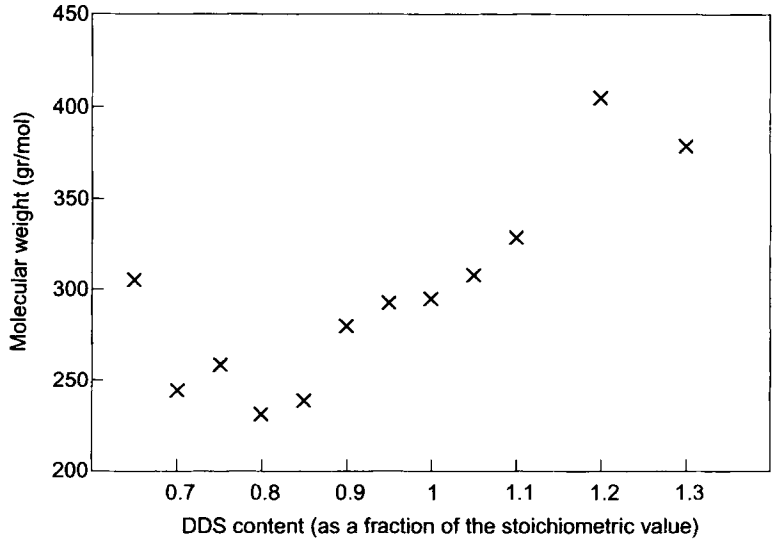


**Figure 4** Average molecular weight between the epoxy network crosslinks ($\overline{M_c}$) as a function of the DDS concentration.

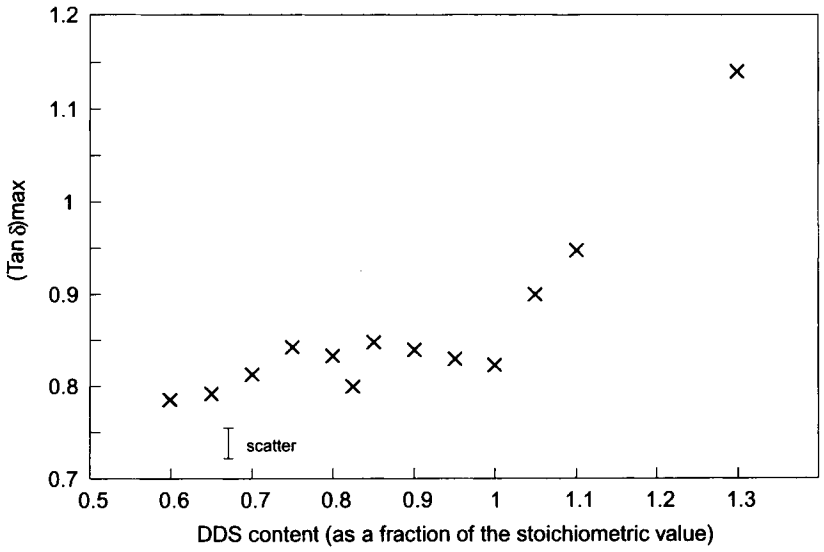


**Figure 5** Variation of the maximum tan $\delta$ peak height, $(\tan \delta)_{max}$, at glass transition of the epoxy network as a function of the DDS concentration.

concentration of the curing agent DDS, and/or cure temperature. Table I shows that increases in curing agent concentration (0.8–1.3) resulted in a decrease in the average value of the ultimate heat of cure from 646 to 600 J/g. Little change in these values would be expected if only PA–E and SA–E reactions were taking place during cure, suggesting that the possibility of the consumption of epoxy groups by reactions other than epoxy-amine addition reactions must be greater in amine-deficient formulations. The literature[2,9–11] indicates that on depletion of the PA–E reaction the SA–E and the E–OH reactions become dominant and proceed at approximately the same rate. The E–OH reactions are encouraged by higher cure temperatures and excess epoxy groups whereas the SA–E reactions by high amine concentrations and lower curing temperatures.

Properties based on dynamic mechanical data are

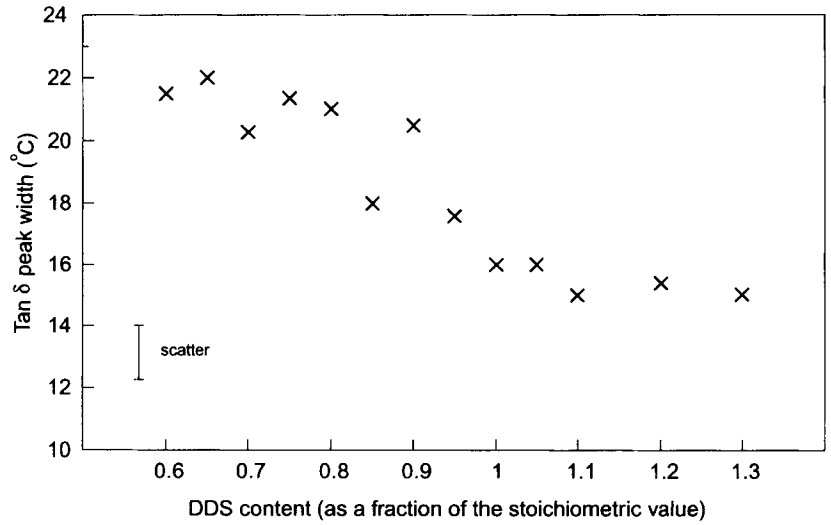


**Figure 6** Variation of the tan $\delta$ peak width at glass transition of the epoxy network with the DDS concentration.

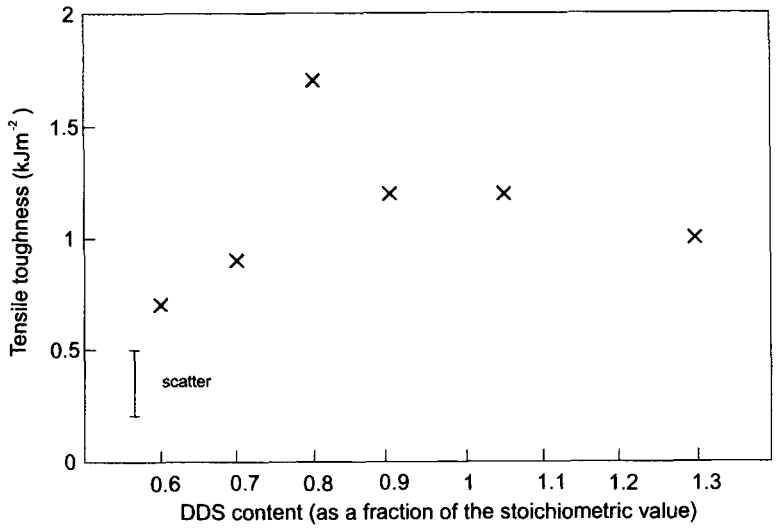


**Figure 7** Variation of the tensile toughness of the epoxy network as a function of the DDS concentration.

presented in Figures 2–6. Figure 3 shows a maximum in the glass transition temperature, $T_g$ (expressed as the temperature of the maximum in the tan $\delta$ peak height at the $\alpha$ transition), which coincides with a maximum in crosslink density or a minimum in molecular weight between crosslinks, $\overline{M}_c$, as shown in Figure 4. The degree of crosslinking is related to the modulus in the rubbery region, $E'$, by the basic theory of rubberlike elasticity such that $\overline{M}_c = 3\rho RT/E'$, where $\rho$ represents the density of the material ($\approx 1220$ kg/m$^3$ for these epoxy–amine systems), $R$ the real gas constant [$\approx 8.315$ J/(mol $\times$ K)], and $T$ the temperature in K. $E'$ values were taken from the DMA storage modulus spectrum at temperatures corresponding to 240–250°C, that is, well above $T_g$, where the rubbery-state equilibrium is assumed. The trends associated with the crosslink density and $T_g$ may be explained in terms of the changing nature of the epoxy–amine network with DDS content. At high DDS contents, curing is

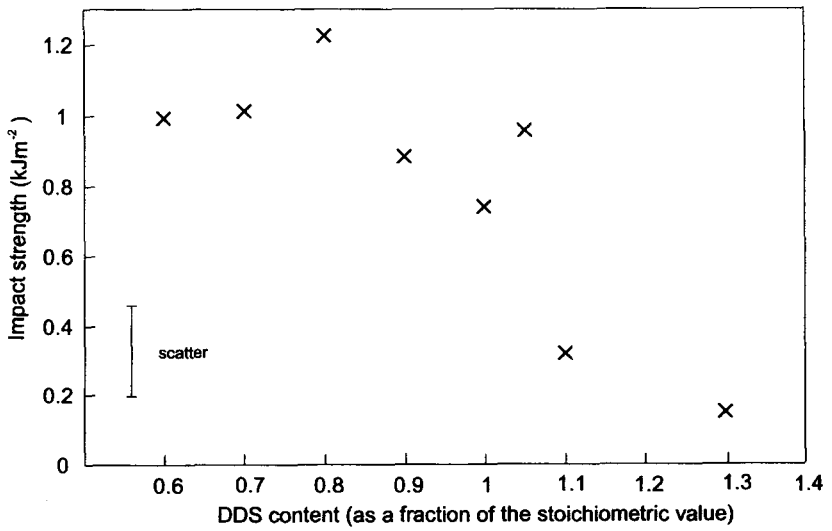


**Figure 8** Variation of the impact strength of the epoxy network with the DDS concentration.

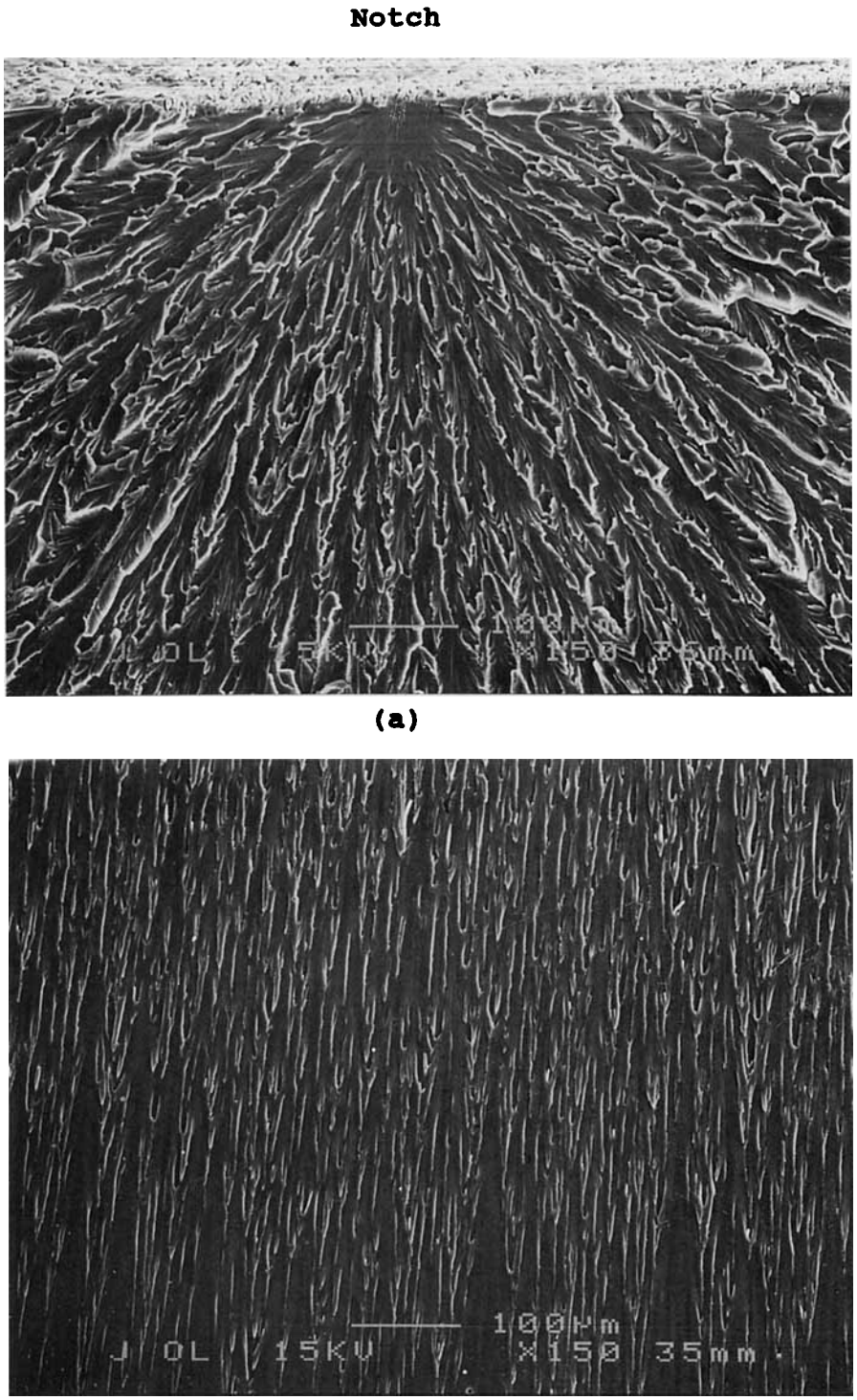


**Figure 9** SEM micrographs of the impact fracture surface of a 0.8 DDS epoxy resin specimen: (a) the fracture initiation and (b) the fracture propagation zones. The bar marker represents 100 $\mu$m.

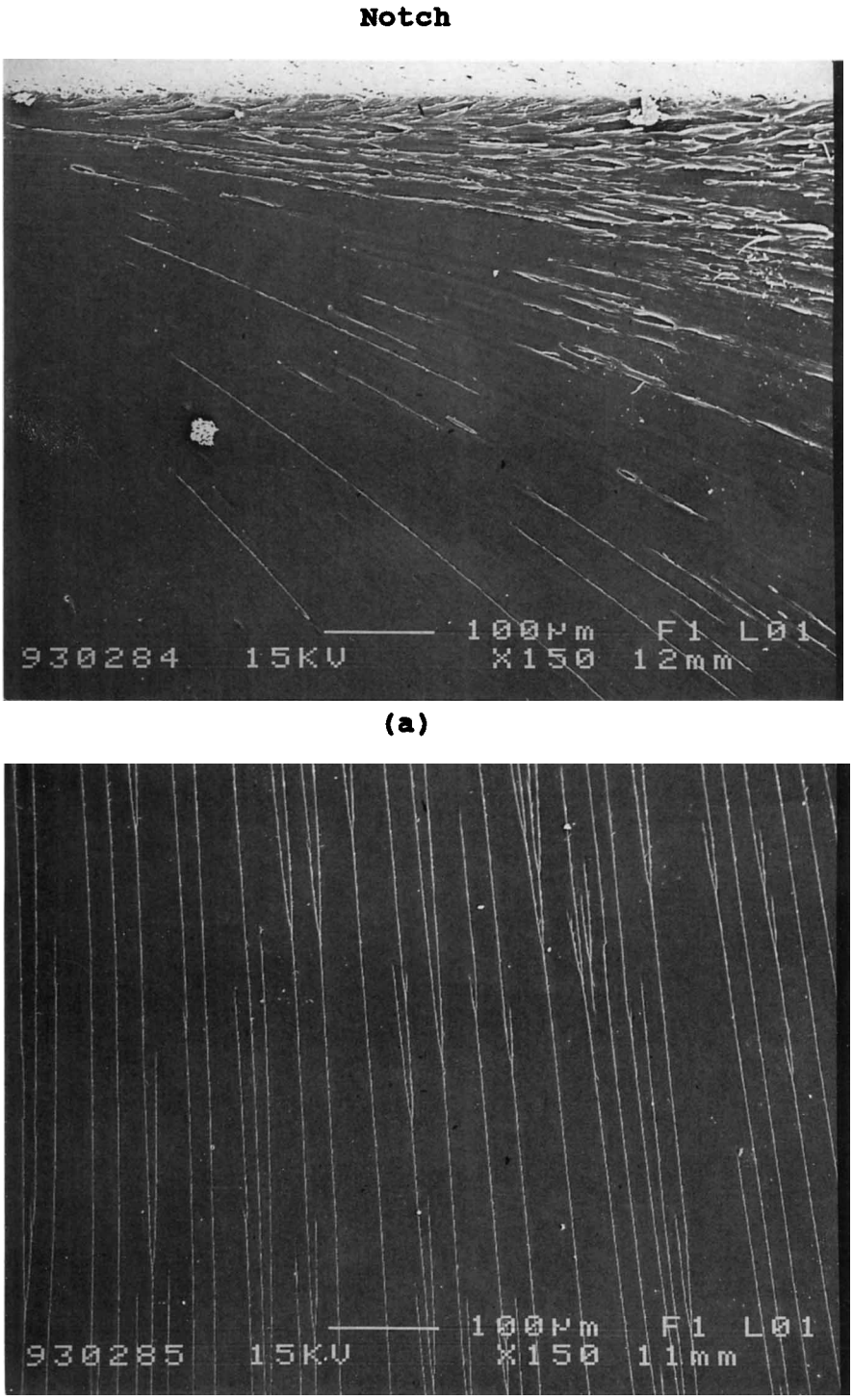


**Figure 10** SEM micrographs of the impact fracture surface of a 1.05 DDS epoxy resin specimen: (a) the fracture initiation and (b) the fracture propagation zones. The bar marker represents 100 $\mu$m.

**Table II Tensile and Impact Properties of PES**

| Elastic Modulus (GPA) | UTS (MPa) | Elongation to Failure (%) | Tensile Toughness ($kJ/m^2$) | Impact Strength ($kJ/m^2$) |
|---|---|---|---|---|
| 2.7 | 87.2 | 6.3 | 47.2 | 4.5 |

mainly by chain extension (i.e., PA–E reactions are dominant) and results in the formation of fewer crosslinks. Increases in tan $\delta$ peak heights with increasing DDS content (see Fig. 5) is also consistent with this suggestion that the degree of crosslinking is lower in amine-rich systems. Formulations containing excess epoxy resin, however, produce broader tan $\delta$ peaks as shown in Figure 6, a manifestation of a more heterogeneous network structure and/or crosslinking as a result of the variety of reactions that may occur during the curing of these formulations, viz. PA–E, SA–E, E–OH, and E–E.

The tensile properties indicated no significant variations with different epoxy formulations and there was considerable scatter in the data. Nevertheless, maximum values were obtained for the area under the tensile stress–strain curve and the impact strength at approximately 0.8 DDS concentration as shown in Figures 7 and 8, respectively. A comparison of the fracture surface micrographs (cf. Figs. 9 and 10) shows that a more detailed fracture surface topography is associated with the higher toughness values.

## Polyethersulphone

The static, impact, and dynamic mechanical properties of PES are detailed in Table II and Figure 11, and the impact fracture surface micrographs featuring ductile tears and "mackerel fracture patterns," also observed in other thermoplastics,[12] are shown in Figure 12. These properties, with the exception of elastic modulus, are superior to those of the epoxy resins by factors of approximately 40 in the tensile toughness, 5 in the impact strength, and 3 in the tensile strength, and by a 20°C increase in $T_g$. Accordingly, PES has been recognized by research workers as a suitable polymer to blend with epoxy resins to impart toughness.

## Epoxy Resin–PES Blends

Epoxy resin–PES blends were prepared at three different DDS contents and at various PES concentrations up to 50% w/w to facilitate the development of a range of morphologies during cure.

### *Curing Behavior*

The plots of the degree of conversion versus time shown in Figure 13 for 0.8 DDS epoxy resin–PES blends highlight certain features common to all the systems considered here: The degree of conversion, at any given time, was decreased with increasing PES concentration and, in the intermediate range of conversion, little difference in the slopes of the curves was apparent at reaction temperatures from

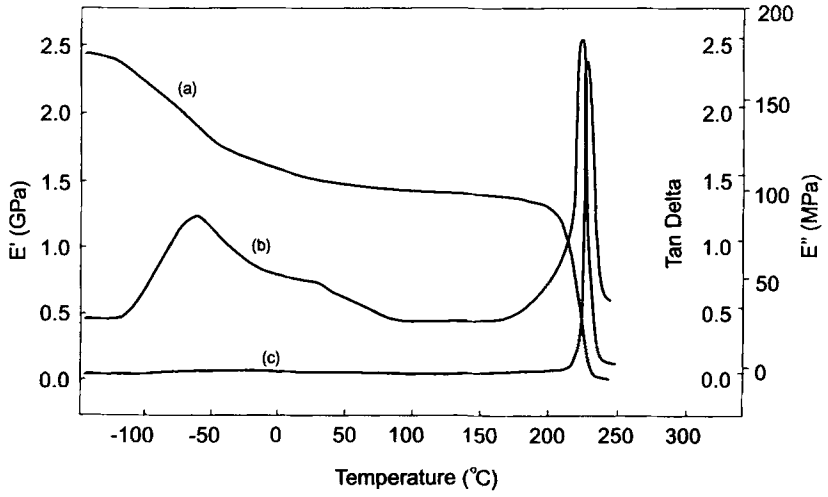


**Figure 11** Dynamic mechanical traces for PES: (a) real modulus ($E'$), (b) loss modulus ($E''$), and (c) tan $\delta$.

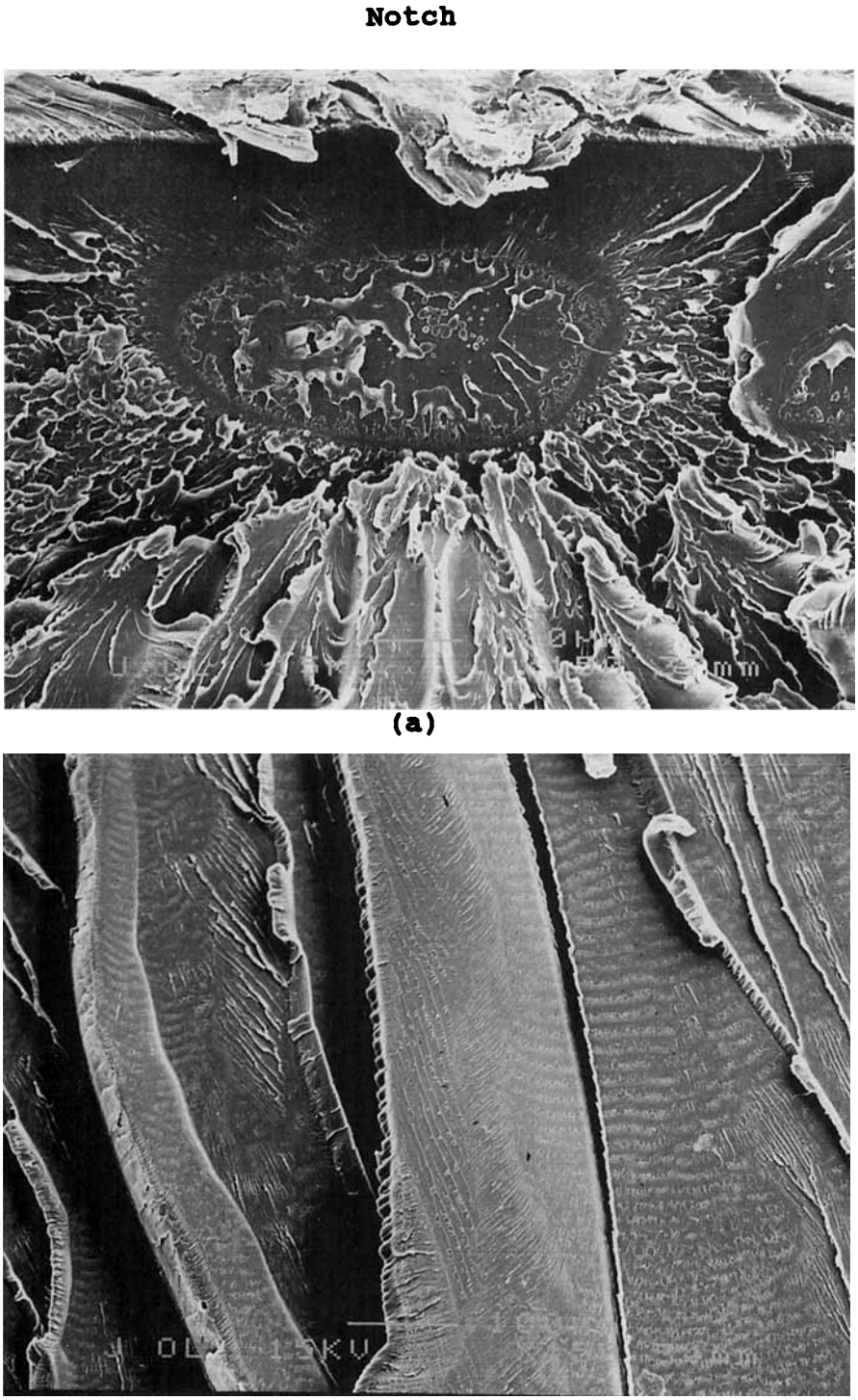


**Figure 12** SEM micrographs of the impact fracture surface of a PES specimen: (a) the fracture initiation and (b) fracture propagation zones. The bar marker represents 100 $\mu$m.

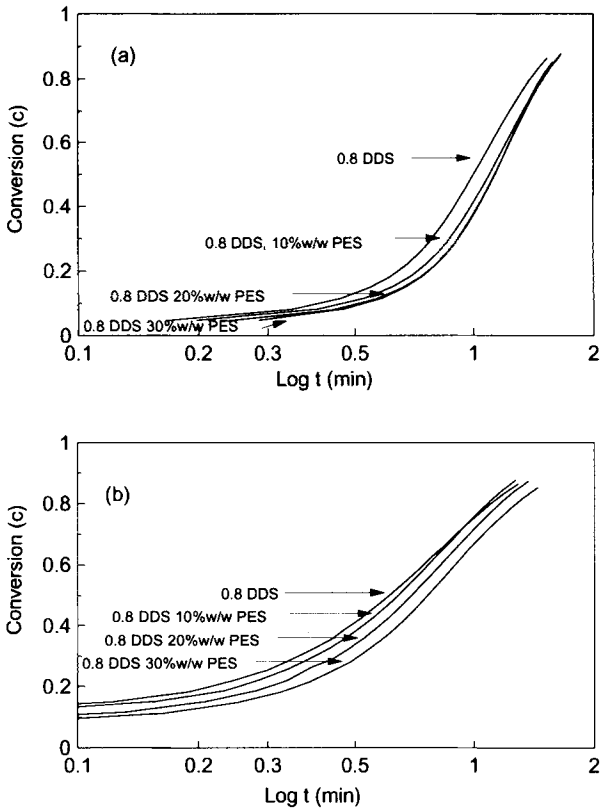


**Figure 13** Degree of conversion vs. log (time) at various PES concentrations for the 0.8 DDS epoxy resin at isothermal cure temperatures of (a) 170°C and (b) 200°C.

145 to 180°C, however, a decrease in the slopes was observed above 180°C.

The plots of reaction rate versus degree of conversion, Figure 14, for the 0.8 DDS resin system at 30% w/w PES exhibits a second exotherm as a shoulder on the main cure profile with a projected reaction rate maximum at approximately 40% conversion. This feature is indicated at high temperatures and/or PES concentrations but diminished with increasing amine content. The presence of the second exotherm in PES-containing systems suggests that PES facilitates the E–OH reaction during cure. It is unlikely, however, that PES has a catalytic effect on the epoxy–amine E–OH reaction since it increasingly depresses the overall rate of reaction as its concentration is increased. It would appear more likely that additional E–OH reaction may be taking place between hydroxyl functional groups in PES and the epoxy groups. Steric and diffusional limitations imposed by the PES on the formation of the epoxy resin–amine network during cure may account for the decrease in the reaction rate with increasing PES concentration. Further details of the curing behavior of these systems are presented elsewhere.[7,8]

### *Morphology*

The nature of the reactions in an epoxy resin–amine/thermoplastic mixture can affect the struc-

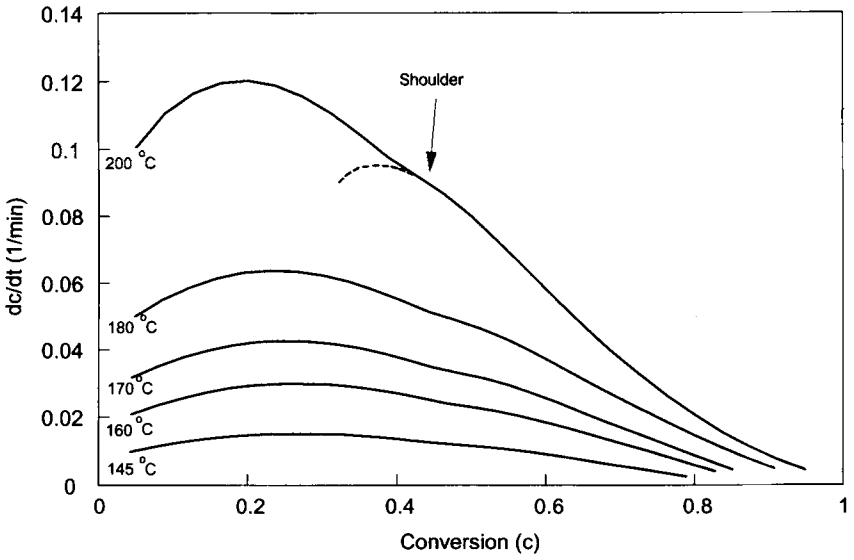


**Figure 14** Reaction rate as a function of degree of conversion for 0.8 DDS epoxy resin/30% PES.

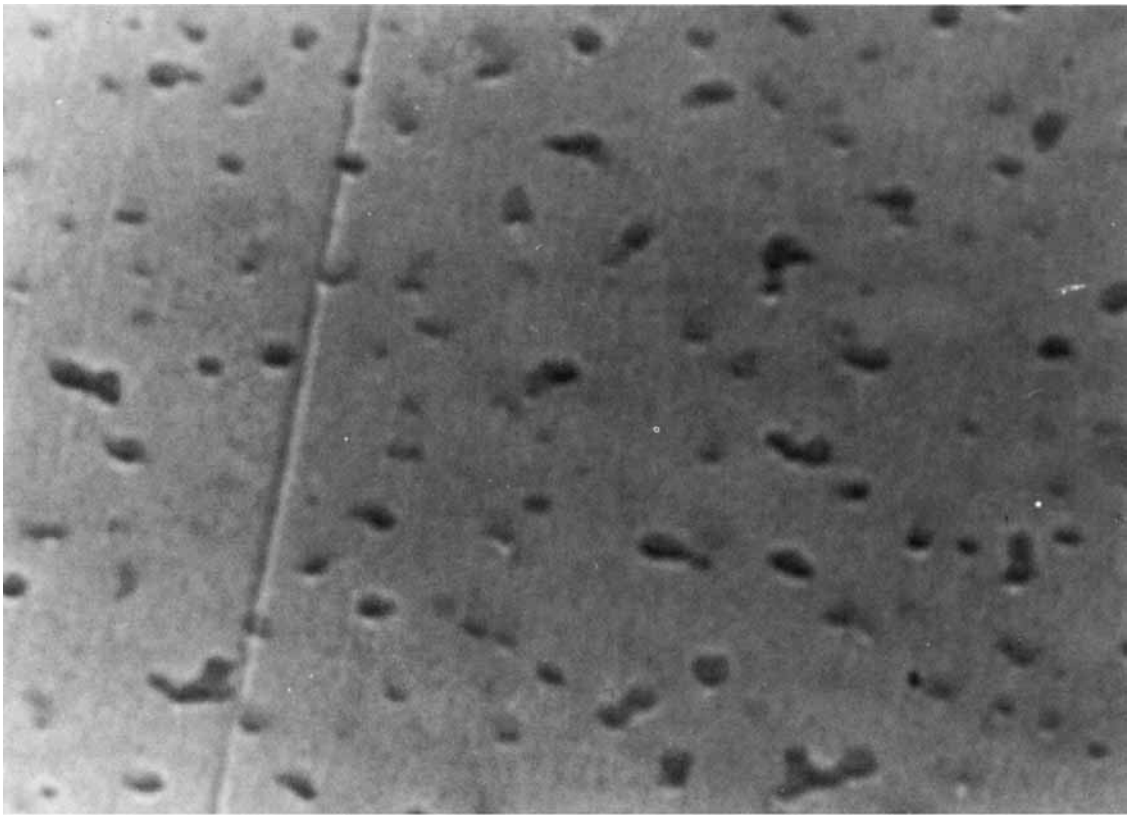

**Figure 15** TEM micrograph of a microtomed section of the 0.8 DDS epoxy resin/10% PES blend. (X30,000 magnification, i.e., 1 mm ≡ 33 nm).

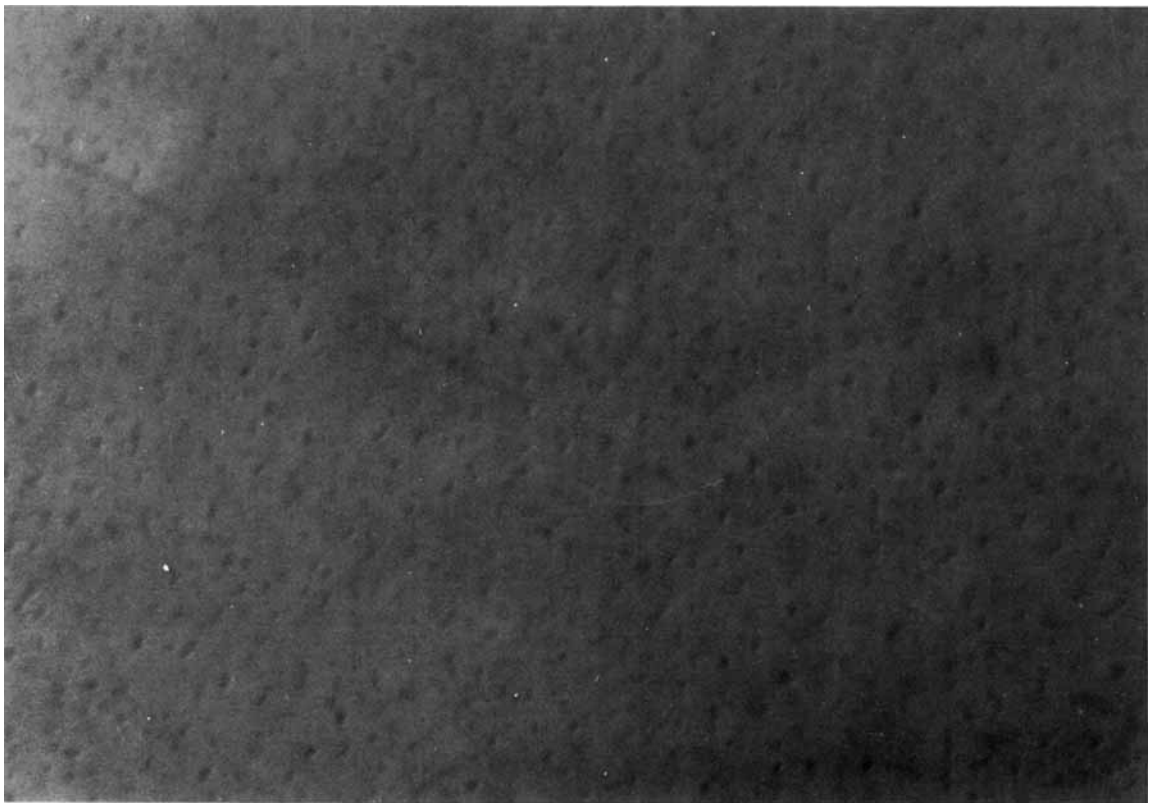

**Figure 16** TEM micrograph of a microtomed section of the 1.05 DDS epoxy resin/10% PES blend. (X30,000 magnification, i.e., 1 mm ≡ 33 nm).

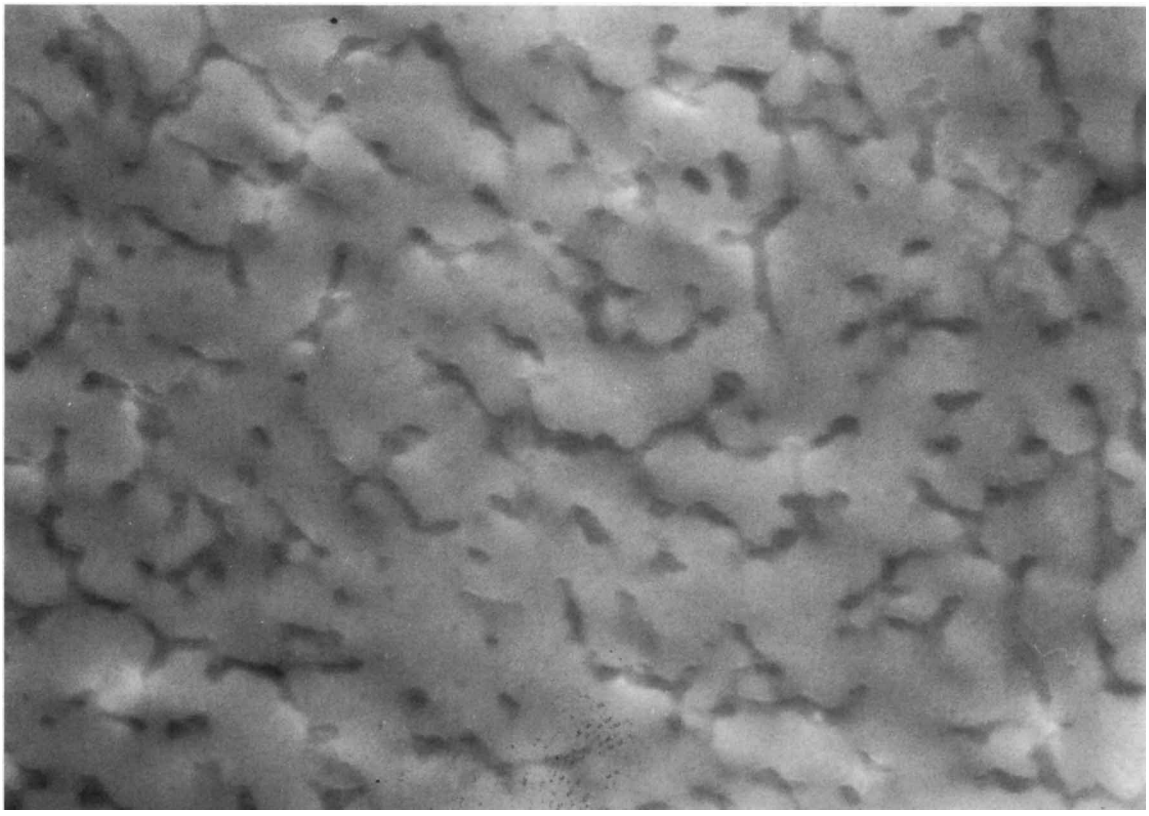

**Figure 17** TEM micrograph of a microtomed section of the 0.8 DDS epoxy resin/20% PES blend. (X100,000 magnification, i.e., 1 mm ≡ 10 nm).

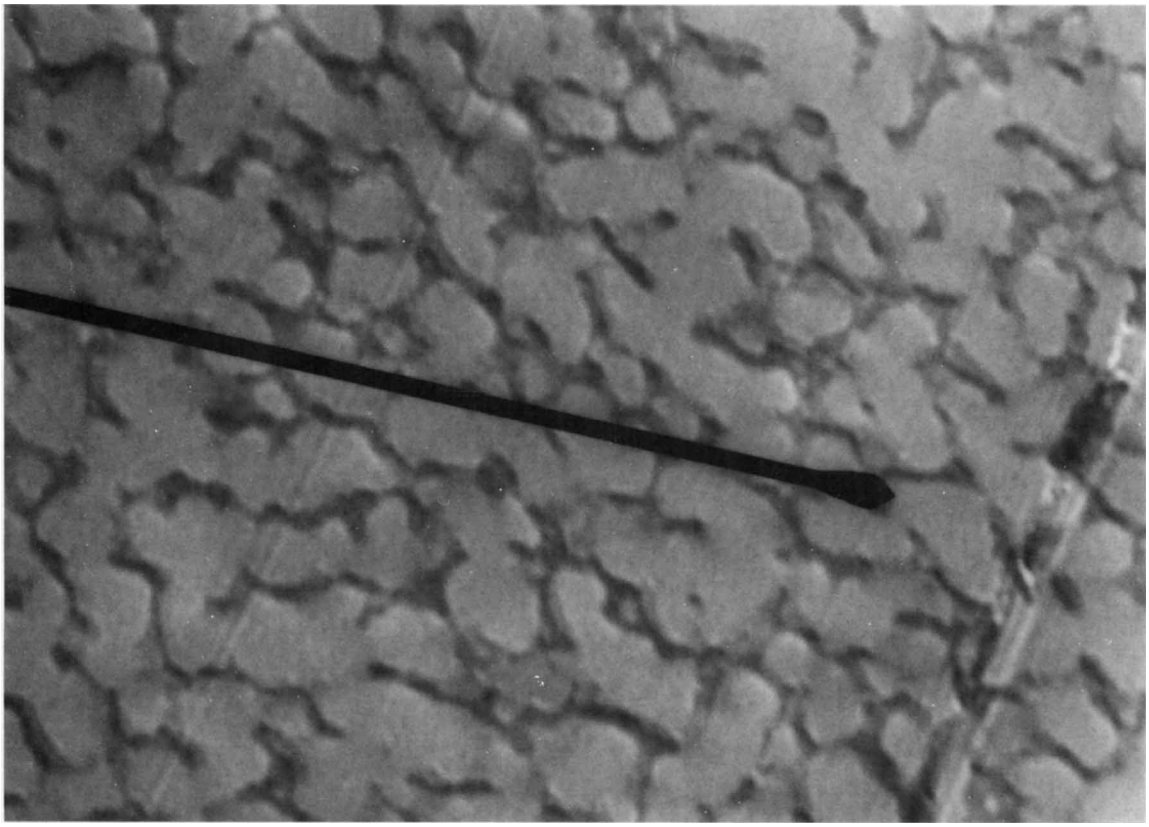

**Figure 18** TEM micrograph of a microtomed section of the 0.8 DDS epoxy resin/30% PES blend. (X30,000 magnification, i.e., 1 mm ≡ 33 nm).

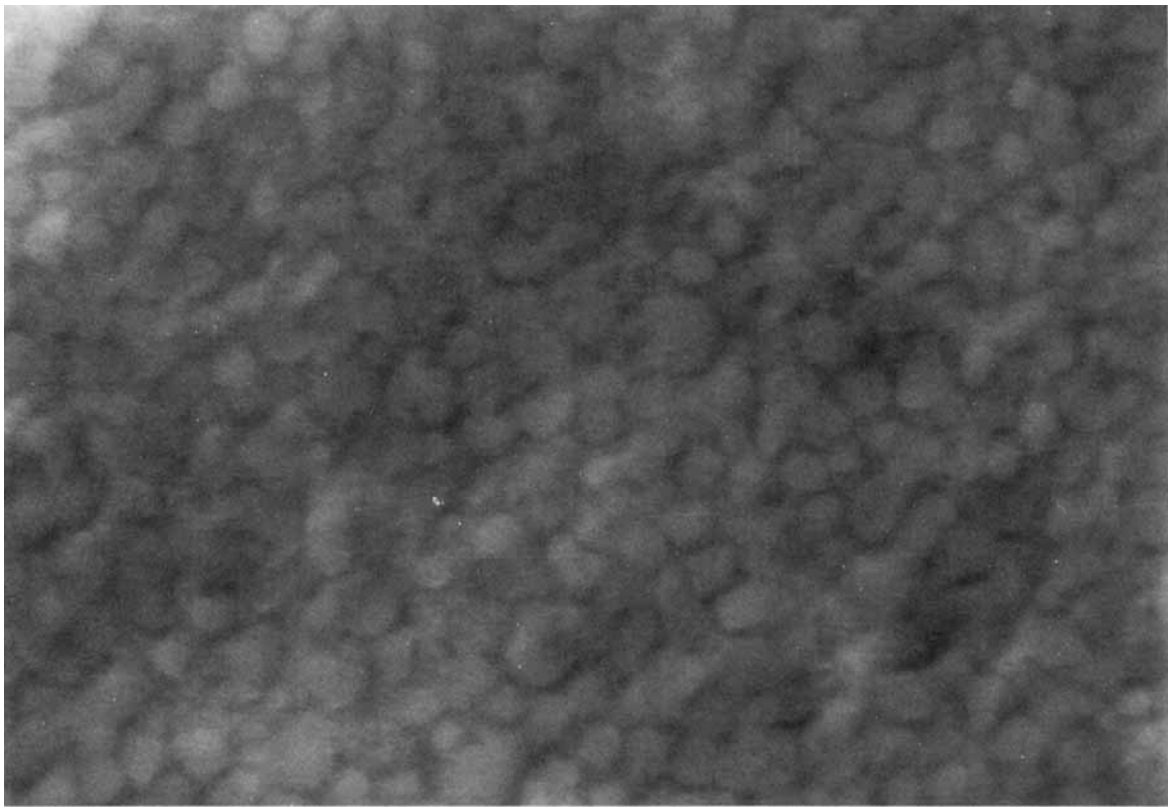

**Figure 19** TEM micrograph of a microtomed section of the 0.8 DDS epoxy resin/40% PES blend. (X30,000 magnification, i.e., 1 mm ≡ 33 nm).

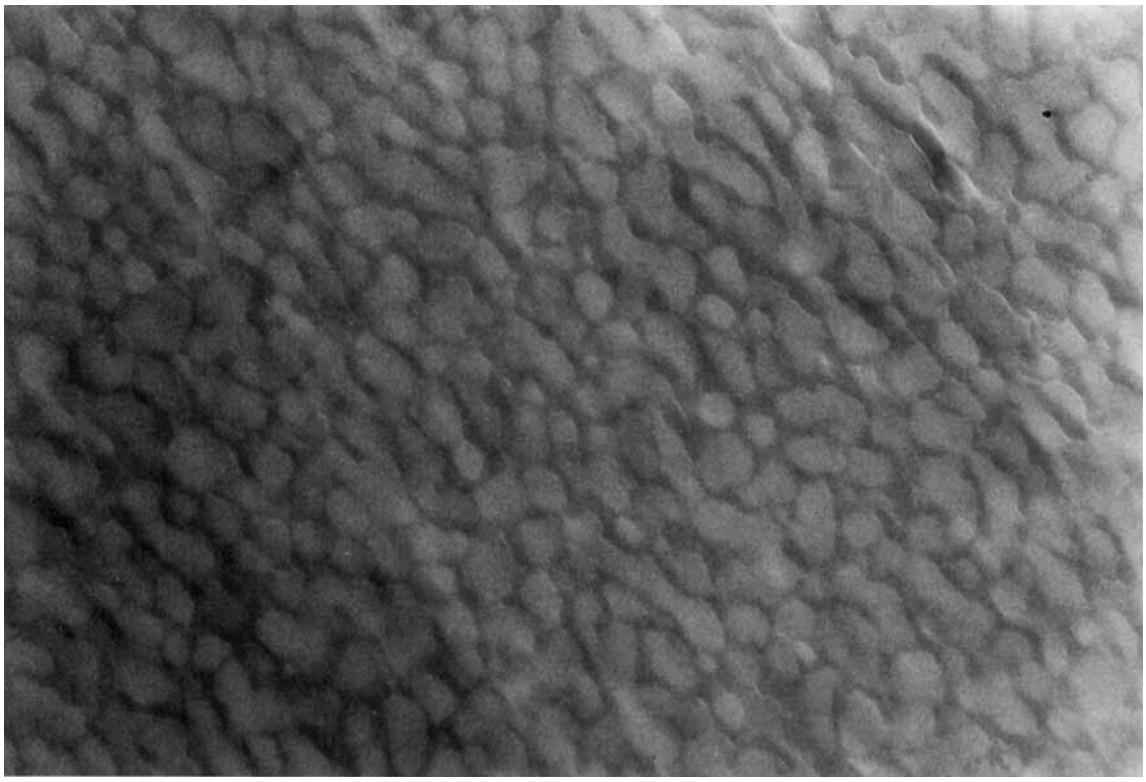

**Figure 20** TEM micrograph of a microtomed section of the 0.8 DDS epoxy resin/50% PES blend. (X30,000 magnification, i.e., 1 mm ≡ 33 nm).

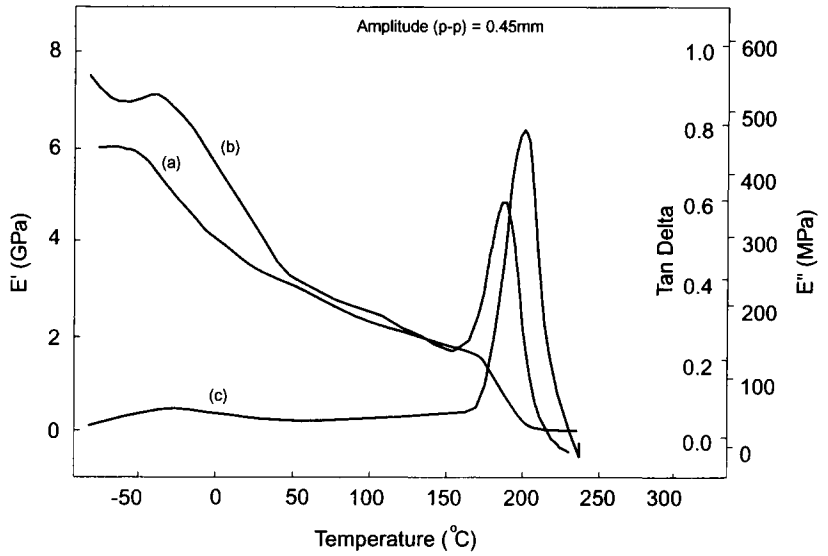


**Figure 21** Dynamic mechanical traces for the 0.8 DDS epoxy resin/30% PES blend: (a) real modulus ($E'$), (b) loss modulus ($E''$), and (c) tan $\delta$.

ture/morphology of the resultant blends. Faster epoxy curing rates, that is, shorter gel times, have been shown to result in finer thermoplastic domains.[13] This is corroborated here: Figures 15 and 16 show that the diameter of the PES phase domains range from approximately 100–150 nm for the 0.8 DDS system to 50 nm for the 1.05 DDS system. It was shown previously that the extent of reaction increases with increasing DDS content.

The morphology of the discrete PES phase within the continuous epoxy phase was observed to change from globules at 10% PES to a spindly, almost fi-

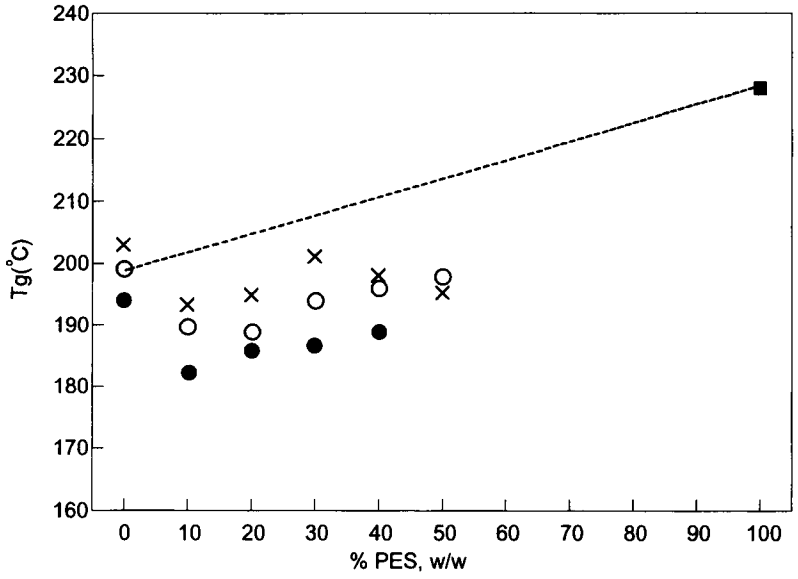


**Figure 22** $T_g$ vs. PES concentration for: (×) 0.8 DDS epoxy resin/PES, (○) 1.05 DDS epoxy resin/PES, and (●) 1.3 DDS epoxy resin/PES blends. (■) 100% PES, (- - -) weighted averages of the $T_g$'s of the component polymers (law of mixture estimates for the $T_g$'s of the blends).

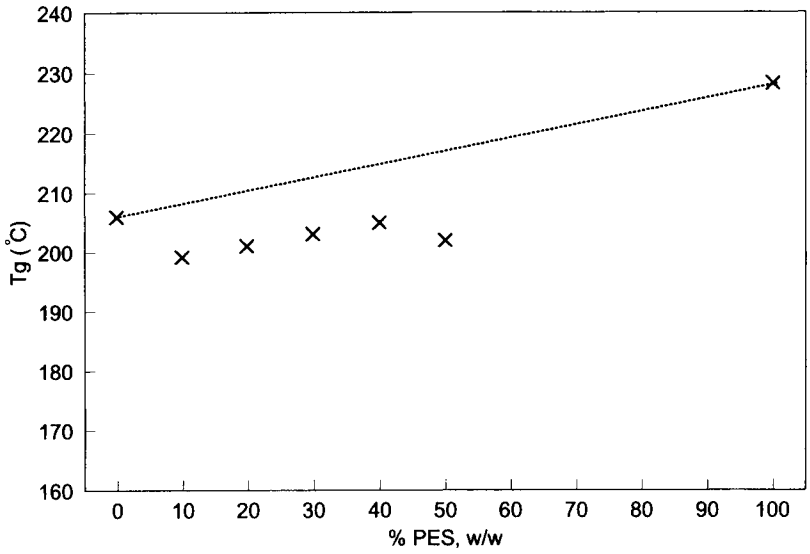


**Figure 23** $T_g$ vs. PES concentration for the postcured 0.8 DDS epoxy resin/PES blends. (– – –) weighted averages of the $T_g$'s of the component polymers.

brous, appearance at 20% PES content (see Fig. 17). A co-continuity was observed at 30% PES as shown in Figure 18, where PES maintains the spindly appearance. Such morphologies have been described as spinodal.[5,14] At 40% PES, the morphology became a mixture of co-continuous and phase-inverted (see Fig. 19). Full-phase inversion can be clearly seen in Figure 20 at 50% PES content, where discrete epoxy resin globules are distributed within the continuous PES phase. Similar morphologies, with some dimensional variations, were observed in different blend systems based on 0.8, 1.05, or 1.3 DDS epoxy resins.

### *Dynamic Mechanical Thermal Behavior*

Figure 21 shows a typical dynamic mechanical thermal spectrum for the blends. The details of any spe-

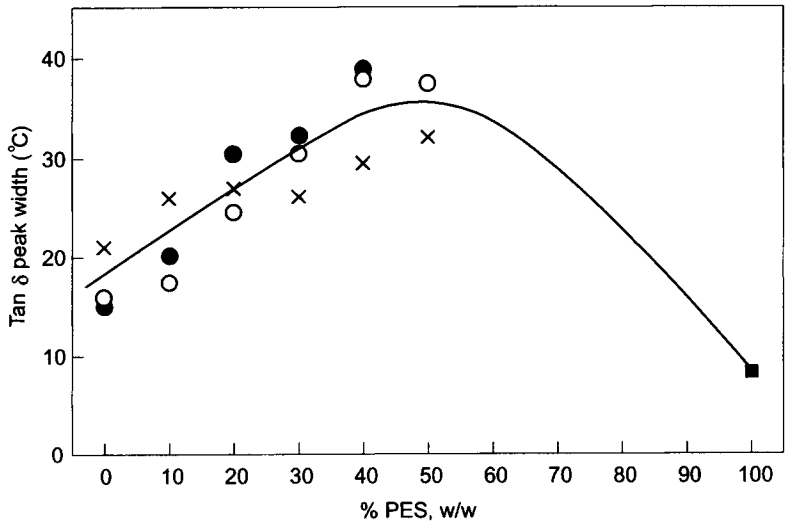


**Figure 24** Glass transition tan $\delta$ peak widths at mid-height vs. PES concentration for: (×) 0.8 DDS epoxy resin/PES, (○) 1.05 DDS epoxy resin/PES, and (●) 1.3 DDS epoxy resin/PES blends. (■) 100% PES.

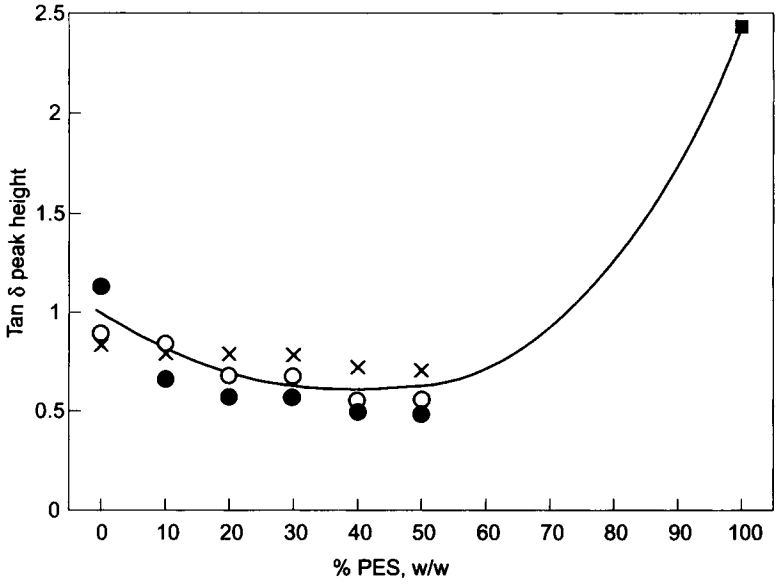


**Figure 25** Tan δ peak heights at the glass transition temperature vs. PES concentration for: (×) 0.8 DDS epoxy resin/PES, (○) 1.05 DDS epoxy resin/PES, and (●) 1.3 DDS epoxy resin/PES blends. (■) 100% PES.

cific differences between the dynamic mechanical properties of the various systems are presented in Figures 22–25. The pattern of change in $T_g$ (expressed as the temperature of the maximum in the tan δ peak height) with increasing PES concentration (see Fig. 22) does not follow any of the standard equations (e.g., Gordon–Taylor,[15] Kelley–Beuche,[16] etc.) for the prediction of the $T_g$ of a polymer blend from the $T_g$'s of the component polymers. The $T_g$'s of the blends were approximately 15°C lower than the values estimated from the component polymers by a law of mixtures relationship. This is assumed as unlikely to arise from plasticization due to any unreacted epoxy monomer or DDS, since the shifts in $T_g$ were observed for all the epoxy resin/DDS ratios considered here even after postcuring as dem-

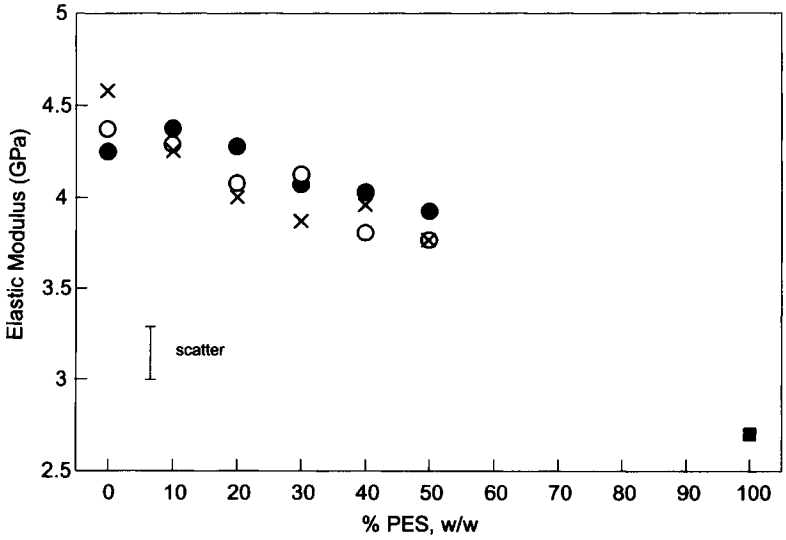


**Figure 26** Elastic modulus vs. PES concentration for: (×) 0.8 DDS epoxy resin/PES, (○) 1.05 DDS epoxy resin/PES and (●) 1.3 DDS epoxy resin/PES blends. (■) 100% PES.

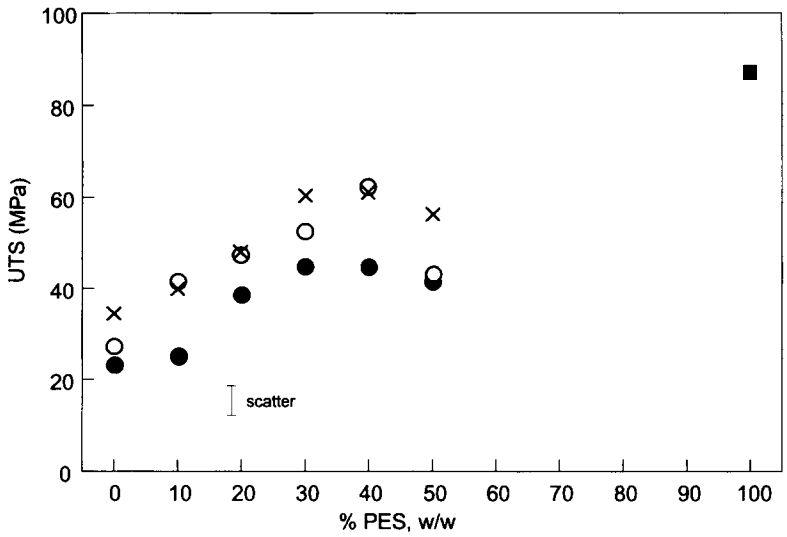


**Figure 27** Ultimate tensile strength vs. PES concentration for: (×) 0.8 DDS epoxy resin/PES, (○) 1.05 DDS epoxy resin/PES, and (●) 1.3 DDS epoxy resin/PES blends. (■) 100% PES.

onstrated in Figure 23 for 0.8 DDS epoxy resin/PES blends (the other blends were almost unaffected by the postcuring treatment). One possible explanation may lie with free-volume effects. It has been shown that blending of polymers generates additional free volume.[17] Increase in free volume can hasten the glass transition by reducing the energy necessary for segmental motion to occur, hence, cause a depression in $T_g$.

Figure 24 shows that the tan $\delta$ peak width broadens with increasing PES concentration; this suggests that a broader free-volume distribution is generated with increasing concentration of the second polymer component (i.e., the minor component polymer).

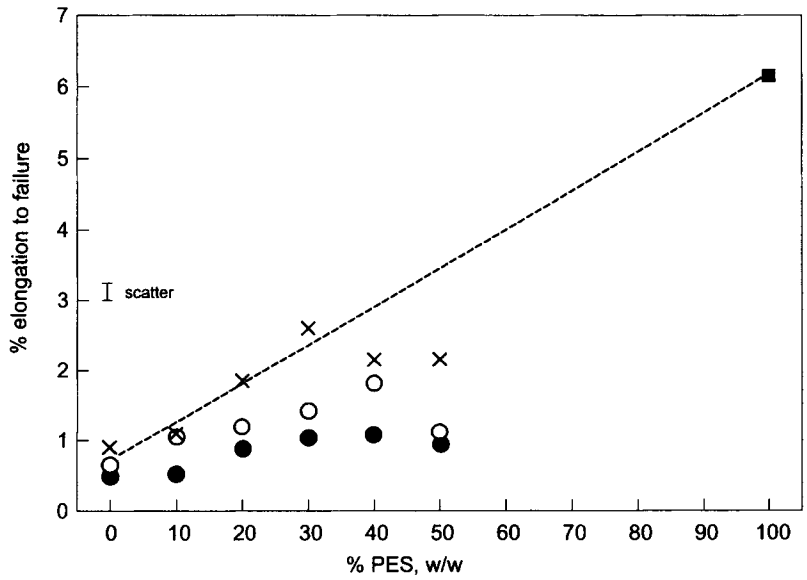


**Figure 28** Elongation to failure vs. PES concentration for: (×) 0.8 DDS epoxy resin/PES, (○) 1.05 DDS epoxy resin/PES, and (●) 1.3 DDS epoxy resin/PES blends. (■) 100% PES, (- - -) weighted averages of the elongations of the component polymers.

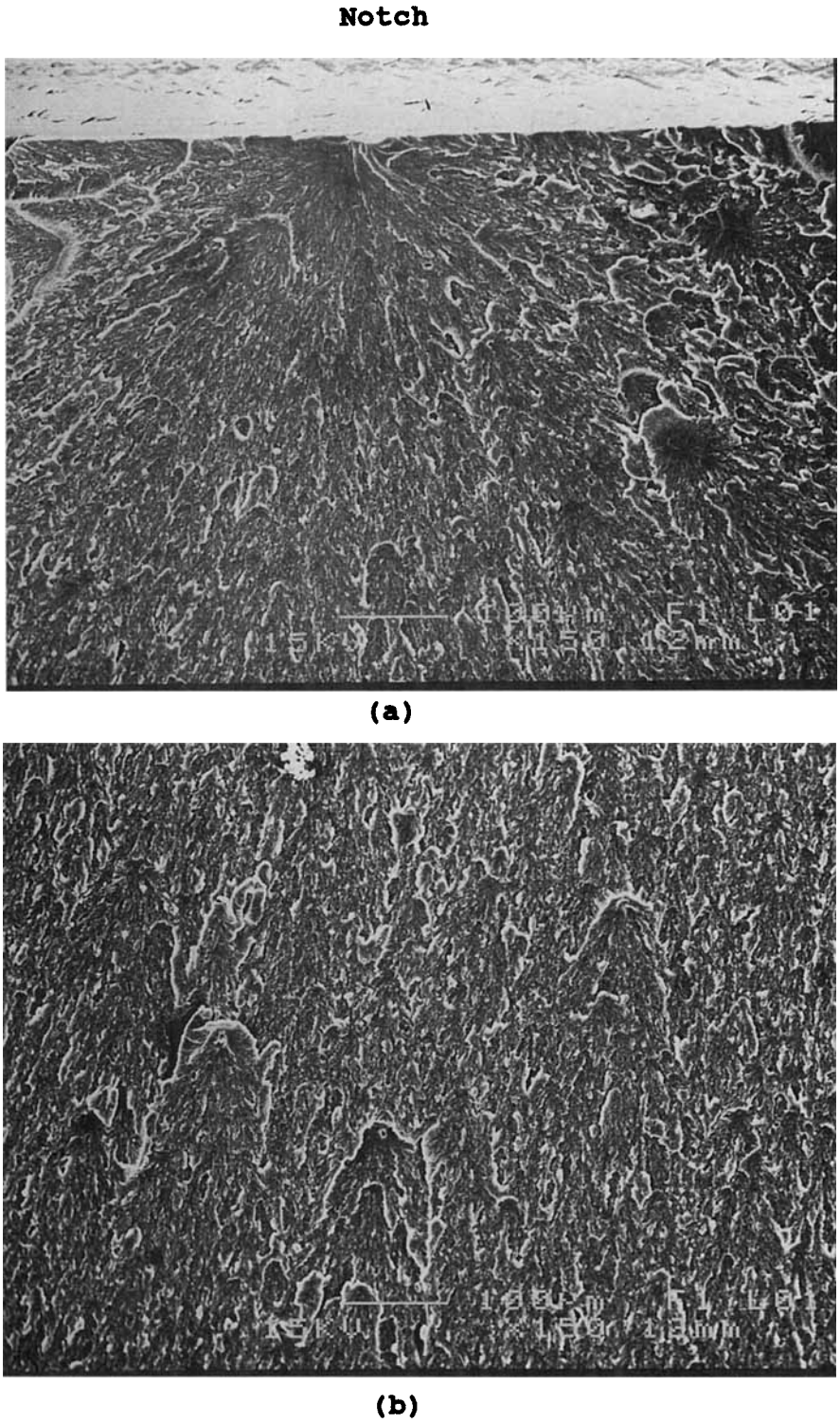


**Figure 29** SEM micrographs of the impact fracture surface of a 0.8 DDS epoxy resin/30% PES blend specimen: (a) the fracture initiation and (b) the fracture propagation zones. The bar marker represents 100 $\mu$m.

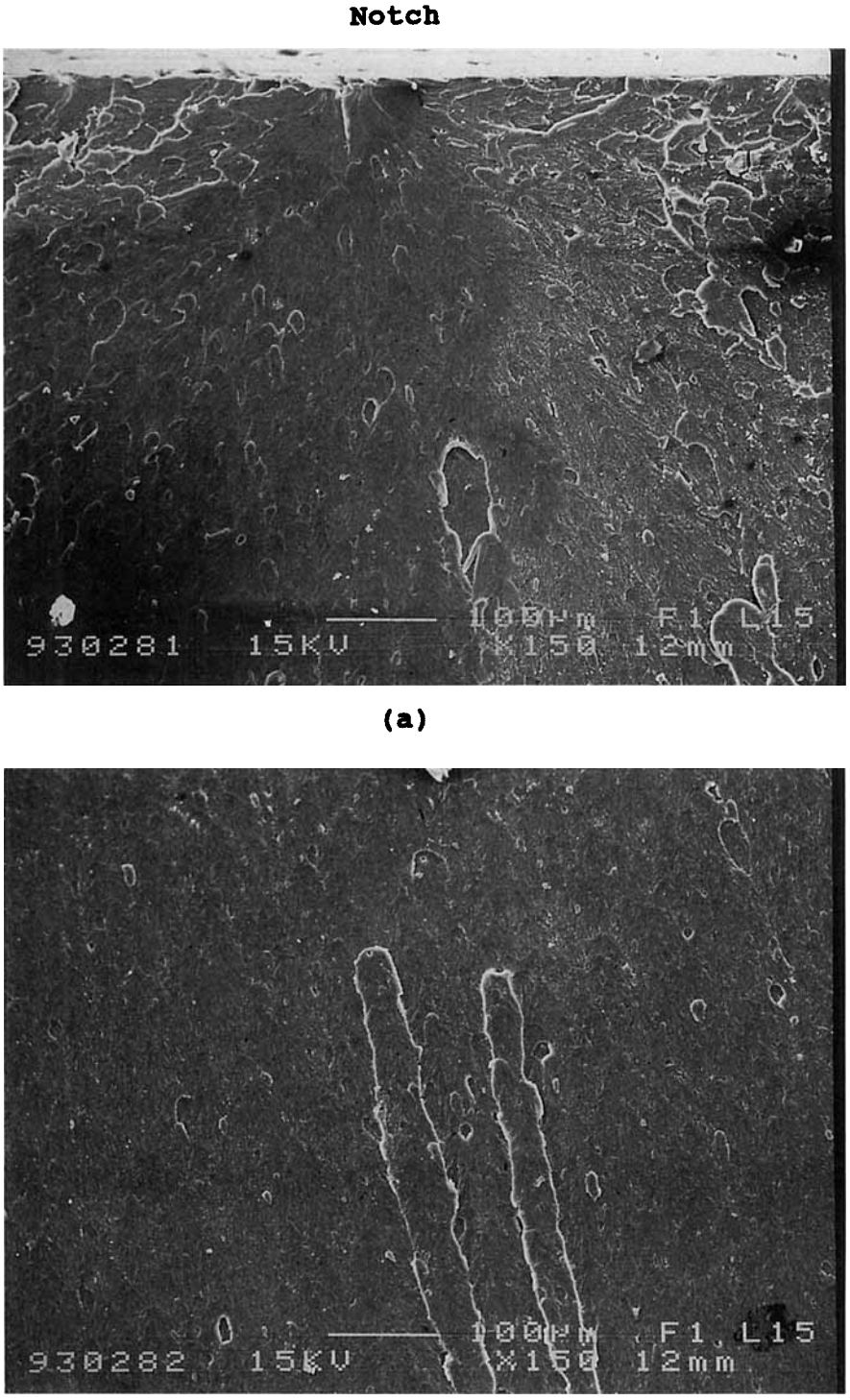


**Figure 30** SEM micrographs of the impact fracture surface of a 1.05 DDS epoxy resin/30% PES blend specimen: (a) the fracture initiation and (b) the fracture propagation zones. The bar marker represents 100 $\mu$m.

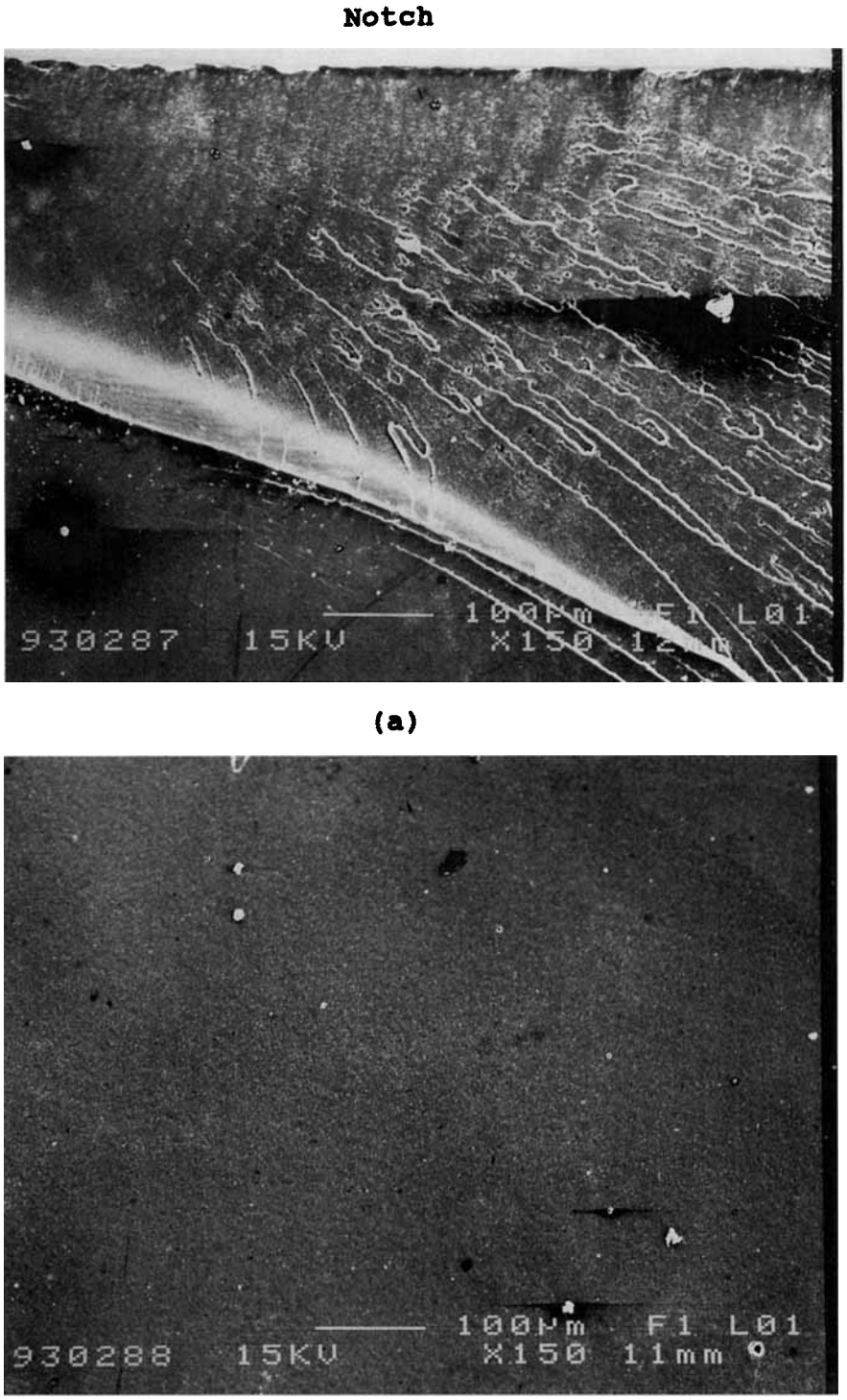


**Figure 31** SEM micrographs of the impact fracture surface of a 1.3 DDS epoxy resin/30% PES blend specimen: (a) the fracture initiation and (b) the fracture propagation zones. The bar marker represents 100 $\mu$m.

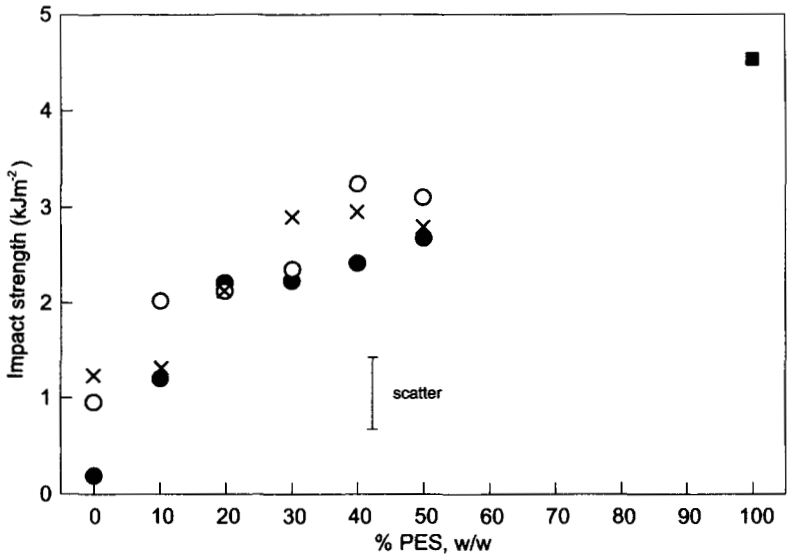


**Figure 32** Impact strength vs. PES concentration for: (×) 0.8 DDS epoxy resin/PES, (○) 1.05 DDS epoxy resin/PES, and (●) 1.3 DDS epoxy resin/PES blends. (■) 100% PES.

**Notch**

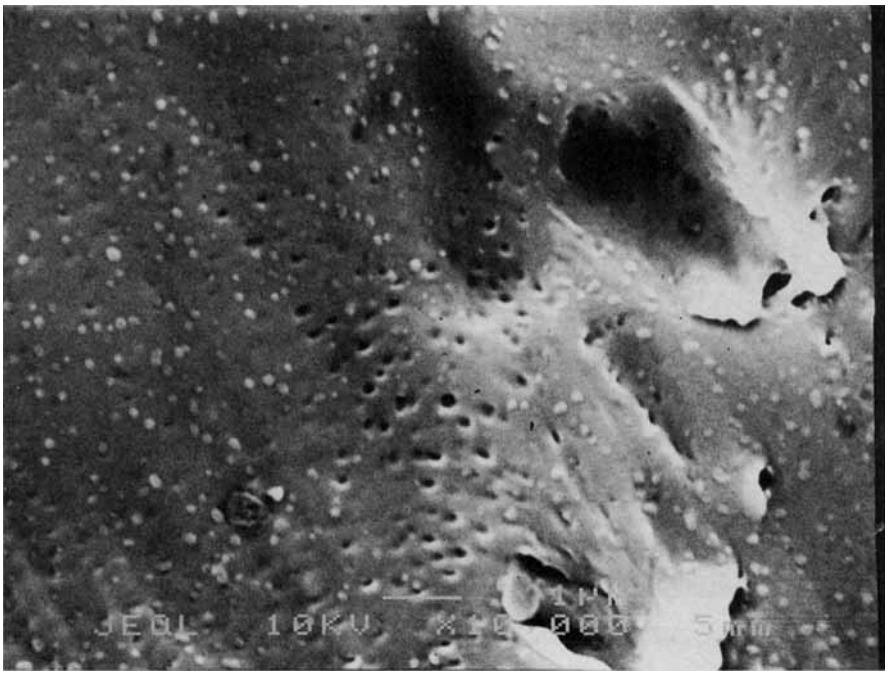

**Figure 33** SEM micrograph of the etched fracture surface of an impact specimen of the 0.8 DDD epoxy resin/10% PES blend. The bar marker represents 1 $\mu$m.

Therefore, it is assumed that the tan $\delta$ peak width registered at approximately equal concentrations of epoxy network and PES is a maximum.

The variation in tan $\delta$ peak height correlates with the amount of the continuous phase present. It decreases with the decreasing epoxy resin content as shown in Figure 25 until the composition level at which PES becomes the continuous phase. Thereafter, the damping characteristics of PES should dominate and increases in tan $\delta$ peak height should ensue with increasing PES content as shown in Figure 25. Similar trends were also observed in polyurethane/poly(methylmethacrylate) interpenetrating networks.[17] Tan $\delta$ peak height, thus, may be used as a convenient indicator of the morphological state of the phases within a blend.

It is also worth noting that the variations indicated in tan $\delta$ parameters as a function of the blend composition were least pronounced in the system based on the epoxy network with the highest crosslink density (i.e., 0.8 DDS epoxy).

### *Mechanical Properties*

The results in Figures 26, 27, and 28 show that as the PES concentration increases in the blends, the elastic modulus decreases, but, ultimate tensile strength (UTS) and percent elongation to failure increase approximately in accordance with a law of mixtures relationship. However, the percent elongation to failure values for the amine-rich formulations fall considerably below the weighted average of the elongations of the component polymers and are consistently lower than the values for the epoxy-rich formulation (i.e., 0.8 DDS epoxy). Elongation at failure is an indicator of the extent of ductility in the material. The impact fracture surface topographies (see Figs. 29, 30, and 31) show that the epoxy-rich system has the greatest ductility. The reason for these improvements are not clear. However, a number of differences, as described below, were indicated between the epoxy-rich and amine-rich formulations: (1) 0.8 DDS epoxy network was shown to have the highest crosslink density (see Fig. 4). Although, this by itself should not result in the observed improvements in ductility and toughness. (2) The occurrence of E–OH and/or E–E reactions in addition to the main curing reactions of E–PA and E–SA, was shown to be more probable during the curing of a 0.8 DDS epoxy resin. Furthermore, the possibility of reaction between the

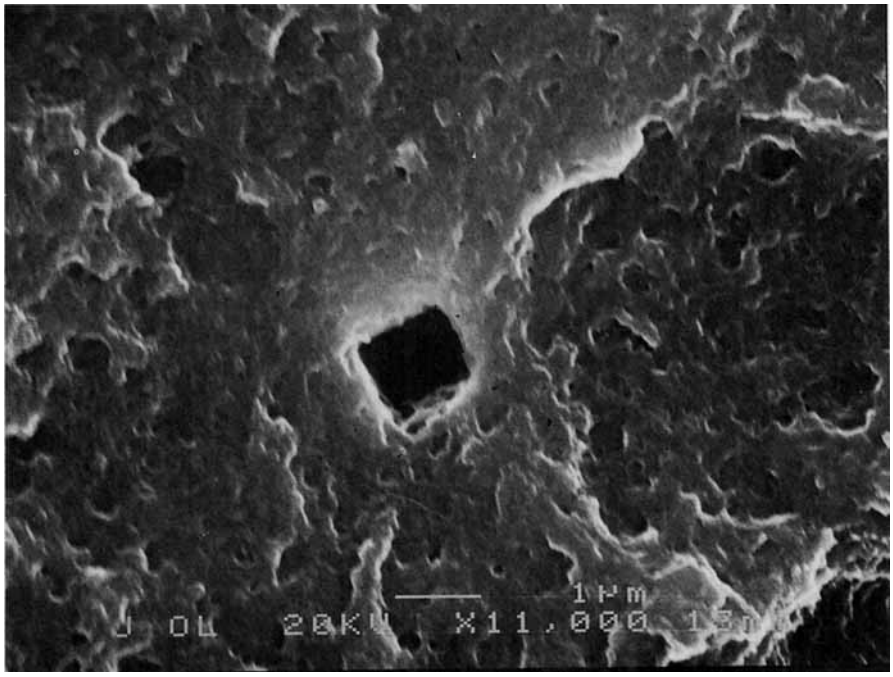


**Figure 34** SEM micrograph of the etched fracture surface of an impact specimen of the 0.8 DDS epoxy resin/40% PES blend. The bar marker represents 1 $\mu$m.

epoxy groups and the OH groups available in PES was also shown to be greater in blends containing excess epoxy resin. (3) The rate of curing is different between the epoxy systems containing 0.8, 1.05, and 1.3 DDS. This influences the extent and size of the phase separation of the component polymers in the blends.

It is probably a combination of these structural variations between the different epoxy networks and between the blends of these epoxy networks with PES that lead to the observed variations in the properties.

The impact strength of the epoxy network/PES blends, as expected, increased with increasing PES content (see Fig. 32). These increases were greater than those indicated by a simple weighted average of the individual polymer values in the composition range 20–40% w/w PES, which corresponds to spinodal/co-continuous morphology. A comparison of the etched fracture surface micrographs (cf. Figs. 33 and 34), where etching has removed the PES component, shows that the epoxy network has a smooth fracture surface at low PES concentrations where the thermoplastic phase separates into discrete particles (see Fig. 33). By contrast, rougher fracture surfaces, see Figures 34 and 35, indicative of more ductile fracture, are associated with co-continuous blend morphologies. The high degree of intertangling between the molecules of the component polymers in the case of co-continuous morphologies probably facilitates a more uniform stress distribution in the material under load and avoids premature failure by localized stress concentration.

The extent of fracture surface roughness is an effective guide to the occurrence of the type of failure. For example, the introduction of a sharp notch by tapping a suitable razor blade at the tip of the blunt machined notch for a 0.8 DDS epoxy resin/30% PES blend caused a more brittle failure with smooth fracture surfaces and nearly straight crack fronts (cf. Figs. 29 and 36).

## CONCLUSION

The curing behavior of an epoxy resin prepared from two parts by weight of triglycidyl-*p*-aminophenol and one part of the polyglycidylether of a phenol-

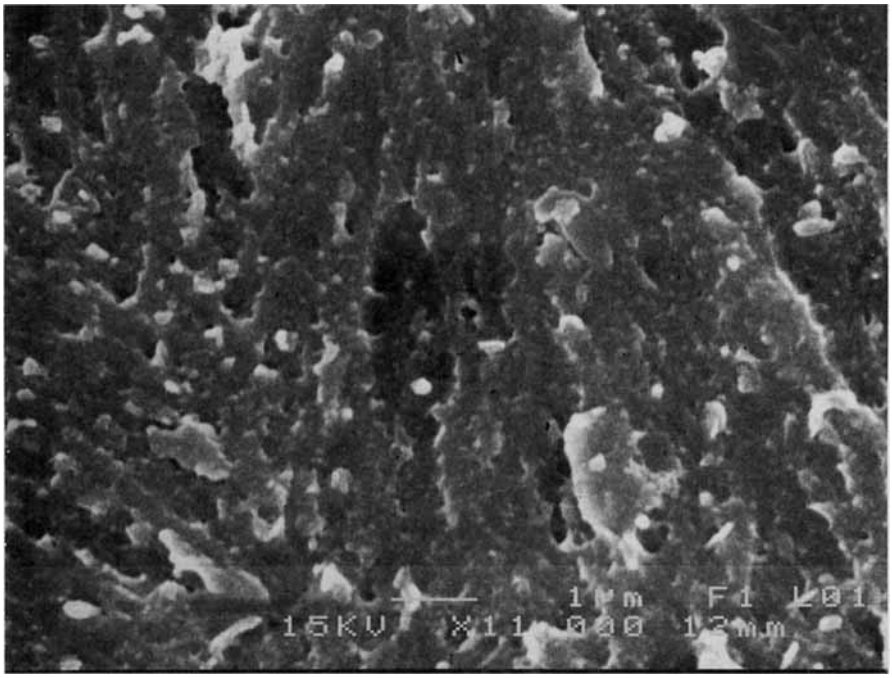


**Figure 35** SEM micrograph of the etched fracture surface of an impact specimen of the 1.3 DDS epoxy resin/30% PES blend. The bar marker represents 1 μm.

Notch

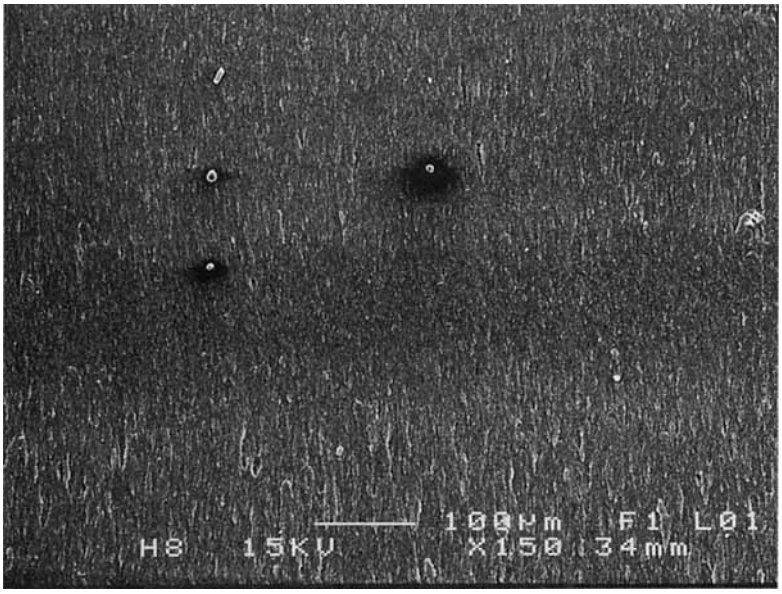


(a)


(b)

**Figure 36** SEM micrographs of the fracture surface of an impact (sharp notch) specimen of the 0.8 DDS epoxy resin/30% PES blend. The bar marker represents 100 $\mu$m.

formaldehyde novolac together with an amine curing agent, 3,3′-diaminodiphenylsulphone (DDS), shows a significant dependence on the curing agent concentration. The maximum degree of crosslinking is obtainable at a lower than stoichiometric amount of curing agent (approximately 0.8 DDS/epoxy). The excess epoxy-rich formulations also seem to facilitate a wider variety of reactions than the amine-rich formulations, generating perhaps more heterogeneous networks.

Incorporation of polyethersulphone (PES) reduces the overall extent of the curing reaction and in sufficient concentration ($\geq$ 30% PES) produces a second reaction exotherm at approximately 40% conversion, particularly in epoxy-rich systems. This is attributed to a possible reaction between the epoxy resin and the hydroxyl groups attached to PES and becomes a further source of variation in network structures, depending on DDS concentration.

The dimensions and morphologies of phases in epoxy resin/PES blends are controlled by the rate of the curing reaction and more significantly by the blend composition.

End-use properties of both 100% epoxy networks and epoxy resin/PES blends are sensitive to structural and morphological variations. Epoxy networks indicated improvements in the glass transition temperature ($T_g$) and in ductility/toughness related properties at a DDS/epoxy resin ratio of 0.8.

The $T_g$'s of the blends are approximately 15°C lower than the values indicated by a law of mixtures relationship. This is attributed to an increase in free volume as a result of blending. Tan $\delta$ peaks at the glass transition become broader and decrease in height with increasing PES concentration up to 50% PES. A reversal of these trends is expected at higher concentrations of PES, where phase inversion is completed and the thermoplastic becomes the continuous phase. The magnitude of changes in tan $\delta$ are least pronounced in the blends based on a 0.8 DDS epoxy network.

Blending-induced improvements in ductility and toughness related properties such as the percent elongation to failure, tensile toughness, and impact strength are noticeably greater in the materials based on an amine-deficient epoxy formulation, viz. 0.8 DDS epoxy resin. Maximum improvements, particularly in impact strength, are indicated at an epoxy network/PES composition range of approximately 80/20 to 60/40, coinciding with a spinodal/co-continuous blend morphology.

We are grateful to ICI Advanced Materials at Wilton, particularly to Dr. P. T. McGrail for supporting the project; and we would also like to thank our colleague Mr. J. E. Riordan for his helpful suggestions.

## REFERENCES

1. J. Mijovic, J. Kim, and J. Slaby, *J. Appl. Polym. Sci.*, **29,** 1449 (1984).
2. R. J. Morgan, J. A. Happe, and E. T. Mones, 28th National SAMPE Symposium, April 12–14, 1983.
3. J. Moacanin, M. Cizmecioghlu, F. Tsay, and A. Gupta, *Organic Coatings and Applied Polymer Science Proceedings, ACS,* **47,** 587 (1982).
4. R. S. Raghava, 28th National SAMPE Symposium, April 12–14, 1983.
5. M. S. Sefton, P. T. McGrail, J. A. Peacock, S. P. Wilkinson, R. A. Crick, M. Davies, and G. Almen, 19th International SAMPE Technical Conference, October 13–15, 700, 1987.
6. D. J. Hourston and J. M. Lane, *Polymer,* **33,** 1379 (1992).
7. J. G. Cracknell, D. Phil. Thesis, University of Ulster at Jordanstown, N. Ireland, 1993.
8. J. G. Cracknell and M. Akay, *J. Thermal Anal.,* **40,** 565 (1993).
9. E. B. Stark, A. M. Ibrahim, and J. C. Seferis, 28th National SAMPE Symposium, April 12–14, 1983.
10. R. B. Prime, *Thermal Characterisation of Polymeric Materials,* E. Turi, Ed. Academic Press, New York, 1982.
11. M. Ochi and J. P. Bell, *J. Appl. Polym. Sci.,* **29,** 1381 (1984).
12. B. Hartmann and G. F. Lee, *J. Appl. Polym. Sci.,* **23,** 3639 (1979).
13. C. B. Bucknall and T. Yoshi, *Brit. Polym. J.,* **10,** 53 (1978).
14. M. Malone, J. Katsaros, F. Karasz, Y. Gur, G. Reynolds, A. Hanson, and E. Riseman, ANTEC '88, 46th Annual Technical Conference and Exhibition, 1174, 1988.
15. M. Gordon and J. S. Taylor, *J. Appl. Chem. (London),* **2,** 493 (1952).
16. F. N. Kelley and F. J. Bueche, *J. Polym. Sci.,* **50,** 549 (1961).
17. M. Akay and S. N. Rollins, *Polymer,* **34,** 1865 (1993).

*Received July 14, 1993*
*Accepted October 27, 1993*